Carbohydrate Polymers 102 (2014) 537–542

Contents lists available at ScienceDirect

Carbohydrate Polymers

journal homepage: www.elsevier.com/locate/carbpol

Dispersion study of nanofibrillated cellulose based poly(butylene adipate-co-terephthalate) composites

Tapasi Mukherjee[a,*], Michael Czaka[a], Nhol Kao[a], Rahul K. Gupta[a], Hyoung Jin Choi[b], Sati Bhattacharya[a]

[a] Rheology and Materials Processing Centre, School of Civil, Environmental and Chemical Engineering, RMIT University, Melbourne, Victoria 3001, Australia
[b] Department of Polymer Science and Engineering, Inha University, Incheon 402-751, Republic of Korea

ARTICLE INFO

Article history:
Received 12 August 2013
Received in revised form 5 November 2013
Accepted 27 November 2013
Available online 4 December 2013

Keywords:
Nanofibrillated cellulose (NFC)
Poly(butylene adipate-co-terephthalate) (PBAT)
Bionanocomposites
Rheology
Nanocomposites

ABSTRACT

The production of lower cost bionanocomposites based on nanofibrillated cellulose (NFC) is a promising source to develop the next generation of light weight and high performance materials for a variety of defense, infrastructure and energy applications. In this study, a series of bio-nanocomposites were developed by reinforcing NFC from regenerated wood fiber into poly(butylene adipate-co-terephthalate) (PBAT) by injection molding. The incorporation of NFC in PBAT matrix (0.2–1 wt%) increased the storage modulus (G') and dynamic viscosity (η') as revealed by shear rheology, indicating a percolation threshold around 0.2–0.5 wt% region. DSC analysis showed similar trends with slight improvement of glass transition (T_g) and crystallization temperature (T_c). Percentage crystallinity, as calculated from heat of fusion equation and taking into account 100% crystallized PBAT data improved in overall. This is a fundamental study aimed at understanding the morphological, rheological and thermal evaluation of such nanocomposites for an improved dispersion of NFC as filler in the matrix.

1. Introduction

Novel bionanocomposites from regenerated wood fiber has experienced increasing interest among researchers during the past decade (Brinchi, Cotana, Fortunati, & Kenny, 2013; Hubbe, Rojas, Lucia, & Sain, 2008; Khalil, Bhat, & Yusra, 2012; Wu, 2012; Siro & Plackett, 2010). The reinforcement from regenerated wood fiber takes the form of isolation of cellulose structures in the nanoscale, leading to the formation of nanofibrillated cellulose (NFC). Some of the unique properties of NFC that serves the material as an ideal candidate for nanofiller include its high strength and stiffness (Yano & Nakahara, 2004; Zadorecki & Michell, 1989), together with transparency (Lavoine, Desloges, Dufresne, & Brass, 2012; Yano, Sugiyama, & Nakagaito, 2005) and biodegradability (Couderc, Duclouz, Kim, & Soumeya, 2009). Typical length and width as reported in the literature for different varieties of NFC as derived, ranges from 500 nm to 2000 nm and 4–20 nm respectively (Moon, Martini, Nairn, Simonsen, & Youngblood, 2011). X-ray diffraction (XRD) study of this variety of cellulose indicates the presence of the crystalline region within a height/width of 4–5 nm and lengths of ~20 nm. The much smaller lengths suggest that either the crystalline regions are longer than that estimated in XRD or they consist of crystalline and amorphous regions arranged in series.

Poly(butylene adipate-co-terephthalate) (PBAT) is an aliphatic–aromatic polyester of butylene glycol and adipic and terephthalic acids and its high percentage elongation (flexible nature) makes it suitable for food packaging and agricultural film application (Averous & Boquillon, 2004). It offers properties similar to low density polyethylene (LDPE) because of its high molecular weight and its branched molecular architecture. It is based on monomers of adipic acid, butanediol and terephthalic acid. Aromatic acid in the polymer reinforces the copolymer structure up to maximum of 40 wt% of terephthalic acid, without changing the biodegradability of the copolyester chains (Raquez, Nabar, Narayan, & Dubois, 2008). The aliphatic part is responsible for its biodegradability. This type of polymer can be synthesized by bulk condensation process and is hundred percent biodegradable. PBAT has excellent softness and ductility. Its mechanical property can be compared to that of low-density polyethylene. Applications of PBAT include food packaging and agricultural film applications (Averous & Boquillon, 2004). However, relatively low tensile strength limits the use of PBAT in large scale applications. Blending PBAT with NFC is the effective way to improve the strength and crystallinity for future biocomposite applications.

* Corresponding author. Tel.: +61 3 9925 2410.
E-mail addresses: tapashi.mukherjee@rmit.edu.au (T. Mukherjee), michael.czaka@rmit.edu.au (M. Czaka), nhol.kao@rmit.edu.au (N. Kao), rahul.gupta@rmit.edu.au (R.K. Gupta), hjchoi@inha.ac.kr (H.J. Choi), sati.bhattacharya@rmit.edu.au (S. Bhattacharya).

0144-8617/$ – see front matter.
http://dx.doi.org/10.1016/j.carbpol.2013.11.047

Although, NFC offers a potential nanoreinforcement to the PBAT matrix, the challenge lies in dispersing them well in the polymer matrix. The inherent fibrillated network structure and the presence of the hydroxyl groups on the surface of NFC limits its dispersion into the polymer matrix. Dispersion is the key factor for an effective nanoreinforcement. Improving the dispersion of the cellulose fibers on the biopolymer matrix is an active area of research interest. Ludvic, Glenn, Klamczynski, and Wood (2007) studied the influence of bentonite clay on the dispersion of cellulose fibers in PBAT and PLA/PBAT matrix. Tensile modulus of the composites improved, while the strength and elongation were impaired due to poor fiber matrix adhesion.

In this study, the degree of dispersion is evaluated by morphological, rheological and thermal tests. TEM analysis indicates an optimal dispersion of PBAT-NFC (0.2 wt%) composite. This uniform dispersion contributed to the shift of glass transition and crystallinity in DSC and enhancement of storage modulus in shear rheological tests.

2. Experimental

2.1. Material

Nanocellulose suspension was procured from Faculty of Forestry, University of Toronto. Poly(butylene adipate terephthalate) was procured from Zhejiang Hangzhou Xinfu Pharmaceutical Co., Ltd. It is similar to the commercial variety Ecoflex FBX7011 by BASF Corp with density of 1.26 g/cm^3 and exhibits a average molecular weight of 143 kDa, polydispersity of 2.46 (GPC analysis), glass transition and melting temperature of −34 °C and 150 °C (Dynamic Mechanical Analysis) respectively, as derived from the technical data sheet.

2.2. Method

Neat PBAT granules were predried in a vacuum oven at 80 °C for 16 h before use. The dried granules of PBAT and the NFC suspension were mixed together at different weight ratios of 99.8/0.2 and 99.5/0.5 in DSM Xplore 15 Micro Compounder for 2 min. The twin screws were maintained at 100 rpm and the processing temperature was set at 140 °C. The melts were then extruded and formed into pellets using the pelletizer.

The pellets of the blended samples were then dried for 16 h before being injection molded. The mixing time of the samples in the Micro-compounder was 2 min. The processing temperature of the twin screws and the transfer device was maintained at 140 °C while the mold ranged from 30 °C to 35 °C. Type 4 specimens were employed to prepare the samples. NFC based PBAT composites of different blend ratios (0.2, 0.5, 0.75 and 1 wt%) were prepared by injection molding technique.

2.3. Characterization

2.3.1. Morphology tests (TEM AFM and XRD)

Morphology of NFC is characterized by transmission electron microscopy (TEM) in a JEOL 1010 instrument at an accelerated voltage of 100 kV. The main purpose of doing a TEM study was to zoom into the nanofibril network to provide clear visualization of ultra-fine morphological development of the entangled nanofibrils. NFC was dispersed in distilled water. A drop of the dispersion was deposited on a carbon-coated TEM grid and allowed to dry prior to imaging.

TEM study on the nanocomposites is performed to characterize the morphology and the dispersion of NFC in the PBAT matrix, and to thereby qualitatively evaluate the interfacial adhesion between the fiber and the matrix. Phillips CM200 (TEM) (Mahwah, NJ) was used to determine the morphology of nanocomposites at an accelerated voltage of 120 kV. Samples were cryosectioned to produce ultra-thin film specimen of 60–80 nm thick, at −170 °C and then placed in a grid for TEM observation. Uranyl acetate (3%) was used as a negative stain for better contrast. Analysis was done using Image J software. Aspect ratio of the fractal network was calculated for objects in several micrographs, taking 20 samples size.

The morphology of NFC was further investigated by atomic force micrography technique. The images (512 × 512) were recorded using scanning rates of 0.250 Hz. The drive frequency and amplitude was 280.02 Hz and 186.0 mV. NFC powder was dispersed in distilled water. A drop of the solution was deposited on a silicon wafer and allowed to dry prior to imaging.

XRD patterns were obtained using a Bruker D4 Endeavor X-ray diffractometer in the angular range of 6–90° (2θ) at a voltage of 40 kV and current of 100 mA. Peak intensities were set up at every 0.02°, at sweep rates of 1.0° 2θ/min, to see the change in crystallinity after addition of NFC to the PBAT matrix if any.

2.3.2. Thermal analysis (DSC and TGA)

The melting and crystallization behavior of the PBAT matrix and their composites were studied using a DSC-2920 (TA Instruments) calibrated with indium with a nitrogen atmosphere, with a flow rate of 35 mL/min. An empty aluminum pan served as a reference. Composite sample weights of approximately 8–10 mg were employed and the samples were encapsulated in an aluminum pan. The samples were heated at 20 °C/min and then cooled at a rate of 5.00 °C/min, respectively in the first heating–cooling cycle. This was done to eliminate any prior thermal history. In the second cycle, samples were cooled to −70 °C, followed by heating to 150 °C at a rate of 10 °C/min.

Glass transition temperature (T_g), melting temperature (T_m), and the heat of fusion (ΔH_m) were taken from the second heating curve. The area under the curve was calculated as the enthalpy from the instrument software. For all the temperature measurements, T_g and T_m are at the onset of the endothermic peak and for T_c, it is at the onset of exothermic peak. The correction for diluents effect linked to the nanocellulose incorporation into the PBAT matrix, as shown in Eq. (1) and Eq. (2) is taken into account to calculate the corrected values of enthalpy, where ϕ is the fraction of cellulose content (Madera-Santana, Drzal, Robledo, & Freile-Pelegrin, 2009).

$$\Delta H'_c = \frac{\Delta H_c}{1-\phi} \quad (1)$$

$$\Delta H'_m = \frac{\Delta H_m}{1-\phi} \quad (2)$$

Thermogravimetry (TGA) was employed to determine thermal stability of PBAT using a Perkin-Elmer TGA-Pyris. Approximately, 2 mg mass of the NFC based PBAT composite was analyzed in an open platinum pan. The sample was heated from 3 °C to 850 °C at 10 °C/min in nitrogen at 20 mL/min. At 700 °C, the gas was switched back to air at 20 mL/min.

2.3.3. Shear rheology

Dynamic frequency sweep tests were conducted using ARES Rheometer (TA Instrument), based on constant strain rate. The tests were conducted using 25 mm parallel plate at temperature of 150 °C. All measurements were performed using a force transducer with a range of 0.2–200 g-cm torque. Prior to any tests, the zero gap between the parallel plates were calibrated at the required temperature. After the sample loading, the test samples were allowed to rest until they reached the temperature (150 °C) at which the rheological measurements were carried out. A delay of 5 min was necessary to erase the thermal and mechanical histories

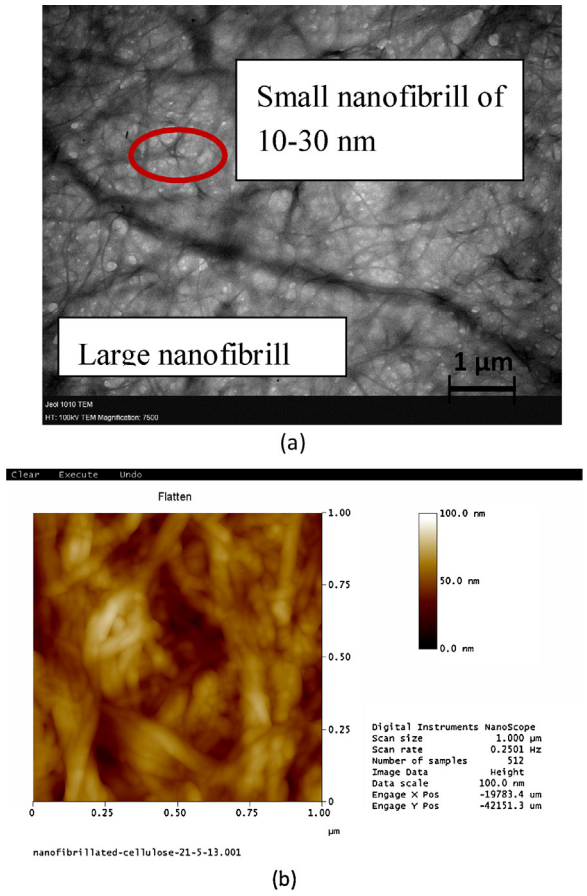

Fig. 1. (a) TEM image of nanofibrillated cellulose network structure. (b) AFM image of nanofibrillated cellulose network structure.

of the sample under investigation. Dynamic Strain Sweeps were conducted at 1, 10 and 100 rad/s at 0.1–100% strain, to check the linear viscoelastic region (LVR) of prepared PBAT/NFC composites at different loading of NFC (0.2, 0.5, 0.75, 1 wt%). A critical strain γ_c was determined at 10 rad/s. Dynamic frequency sweep tests were conducted in the LVR region at 10 rad/s, between the frequency of 0.1 and 100 rad/s at 150 °C.

3. Results and discussion

3.1. Morphological study

Fig. 1(a) and (b) shows the formation of nanofibril network under TEM and AFM imaging. From the imaging, it is apparent that the core structure was formed by the internal fibrillation of submicron nanofibrils of 10–30 nm, to several hundred nanometers, which probably resulted from external fibrillation. Fig. 2(a)–(d) shows the TEM image of PBAT-NFC composite (0.2–1 wt%). From this figure, it is evident that fine dispersion of NFC is apparent at 0.2 wt%. Meanwhile, addition of NFC did not destroy the original structure of PBAT, which is again ensured by the XRD study as discussed in the subsequent sections of this paper. However, with a continuous increase in the loading level of NFC, some conglomerates emerged as shown in Fig. 2(c) and (d), which is mainly attributed to self-aggregation of the superfluous nanofiller. This observation is similar to a study on organomodified clay based PBAT composites, where big agglomerates of micrometer size appear (Bittman, Bouza, Barral, González-Rodríguez, & Abad, 2008). Aspect ratio as determined from this network fractal study on 0.2 wt% NFC composite is ranging from 1 to 2.5.

In XRD analysis, as shown in Fig. 3, neat PBAT exhibited five different diffraction peaks, with a combination of amorphous and crystalline structure. The crystal peaks are observed at 16.4°, 17.4°, 20.6°, 23.2° and 24.7°, similar to the study performed by Chivrac, Pollet, and Averous (2007). Five similar characteristics peaks are also observed at the same values for all PBAT-NFC nanocomposites, except that 0.2 seems rather quantitatively different from others, with significant reduced peaks at 16.4 and 12.4 relative to the other peaks. From these observations, it can be inferred that there is no important transcrystalline phase in the system interface. Therefore there is few or no change in the PBAT crystal structure as induced by nanofiller incorporation.

3.2. Thermal study

Table 1 summarizes DSC results. From the data it is observed that there is a slight shift of the glass transition on addition of NFC to the PBAT matrix reaching its maximum at 0.2 wt% indicating optimal dispersion. The uniform dispersion of the NFC filler restricts the polymer chain mobility, thereby increasing the T_g value. With further loading, agglomeration of NFC starts to begin, due to hydrogen bonding and thereby filler-filler interaction dominates, which eventually decreases the T_g value. The observed value complements morphology study by TEM, where an optimal dispersion was observed at 0.2 wt%. It is also apparent that the corrected values of heat of fusion ($\Delta H'_m$ and $\Delta H'_c$), as calculated from Eq. (1) and Eq. (2), are higher in comparison to the values obtained from the thermograms as the effect of diluent is taken into account in this equation. The corrected values are equivalent and both are into the range of 10.1–15.7 J/g, similar to the study performed by Madera-Santana et al. (2009) on agar based PBAT particles. However, the incorporation of NFC did not induce any significant effect on the crystallization temperature (T_c). The percentage of crystallinity (X_c) increases with increasing content of NFC, which is unlike to the literature reported on clay and natural filler based PBAT composites. This indicates the potential of NFC as a nucleating agent on the PBAT matrix.Thermogravimetry (TGA) was performed to confirm composition and establish thermal stability of PBAT composites in a nitrogen atmosphere. Fig. 4 and Table 2 reflect the mass change and degradation temperatures. As evident from the figure, TGA shows a one-step mass loss that indicates degradation started at approximately 320 °C and was complete by approximately 465 °C, similar to the study performed by Madera-Santana et al. (2009) on agar based PBAT particles. Pure PBAT had a higher decomposition temperature. Adding NFC reduced the decomposition temperature by

Table 1
Summarized DSC data indicating the thermal behavior of PBAT-NFC composite.

NFC	T_g (°C)	ΔH_g (J/g)	T_m (°C)	ΔH_m (J/g)	$\Delta H'_m$ (J/g)	T_c (°C)	ΔH_c (J/g)	$\Delta H'_c$ (J/g)	X_c
0	−33.93 (0.3)	0.23	116.6 (0.5)	7.65	7.65	79.74 (1)	7.53	7.53	6.71
0.2	−25.3 (0.2)	0.2	116.69 (0.6)	11.58	11.60	80.17 (0.6)	9.8	9.82	10.18
0.5	−29.8 (0.2)	0.23	117.47 (0.5)	11.7	11.76	81.66 (0.3)	9.3	9.35	10.32
0.75	−27.34 (0.2)	0.03	115.54 (0.1)	13.53	13.63	82.18 (0.3)	10	10.08	11.96
1	−29.15 (0.3)	1.16	114.68 (0.1)	13.33	13.47	79.27 (0.1)	10.3	10.40	11.81

Note: Values in parenthesis are standard deviation of 5 samples.

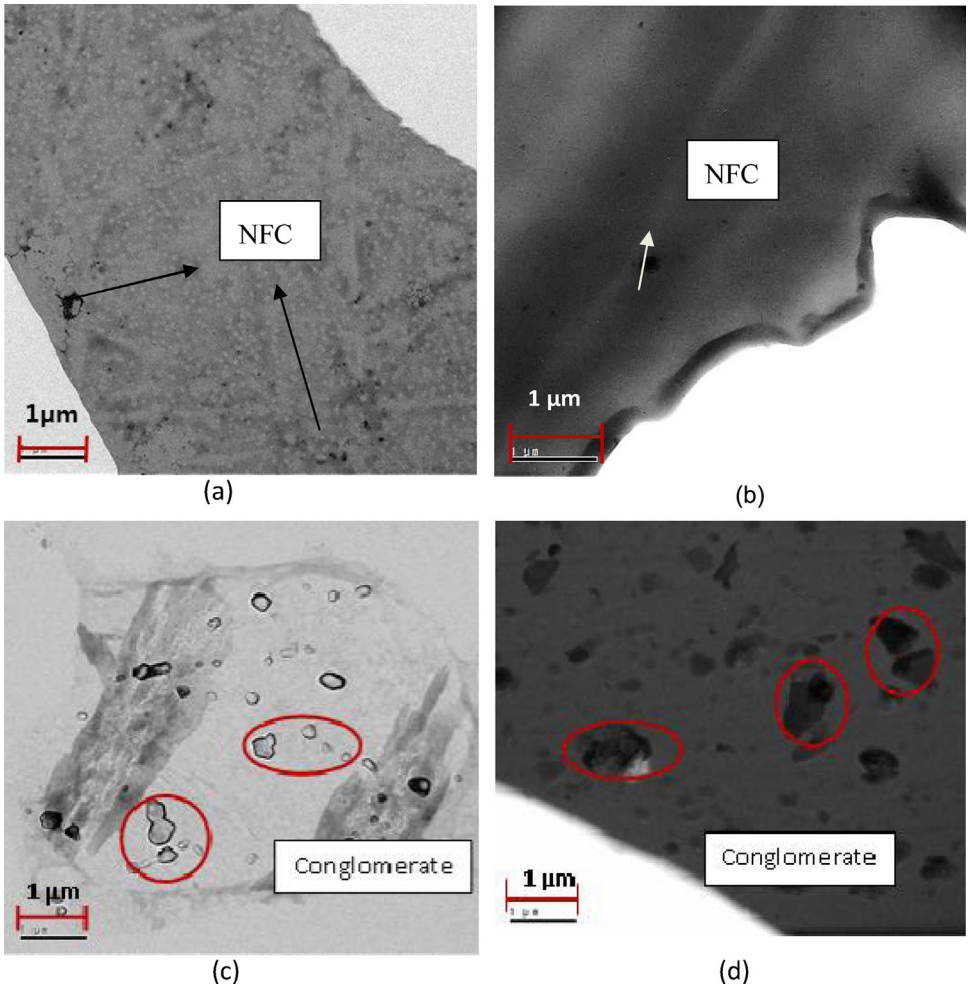

Fig. 2. TEM images of (a) PBAT-NFC (0.2 wt%), (b) PBAT-NFC (0.5 wt%), (c) PBAT-NFC (0.75 wt%) and (d) PBAT-NFC (1 wt%).

1–3 °C, in a non-linear fashion. Notably, the TGA curve showed no other deflection indicating that NFC was well dispersed in PBAT or consisted of too little of the mass to be detected. Thus adding NFC to PBAT only slightly decreased its heat resistance, which is desirable as low heat resistance can make molding, disposal and reprocessing easier.

3.3. Shear rheology

Rheology is an effective way of probing the microstructure and assessing the state of dispersion of the nanocomposites directly in the melt state (Mabrouk, Magnik, Belgacem, & Boufi, 2011). Investigation on dispersion, network formation and microstructural changes of NFC in the PBAT matrix at melt state is performed by oscillatory measurements. Fig. 5(a)–(c) compares the storage modulus (G'), loss modulus (G'') and complex viscosity (η^*) of PBAT-NFC composites at various loadings, ranging from 0.2 wt% to 1 wt% at 150 °C, when subjected to dynamic frequency sweep tests. From these figures, it is evident that the enhancement of storage modulus (G'), loss modulus (G'') and complex viscosity (η^*) is significant at all frequencies for all PBAT-NFC composite in comparison to neat PLA, reaching its optimal value at 0.2 wt%, particularly at the lower frequency range. However, it should be noted here that this enhancement is not proportional to the amount of NFC added. Enhancement of storage modulus reached its optimal value at 0.2 wt% and then decreased with further loadings. This occurrence

Table 2
Summarized degradation temperature of PBAT-NFC composite.

NFC added (%)	Degradation temperature (°C)
0	400
0.2	398
0.5	397
0.75	399
1	398

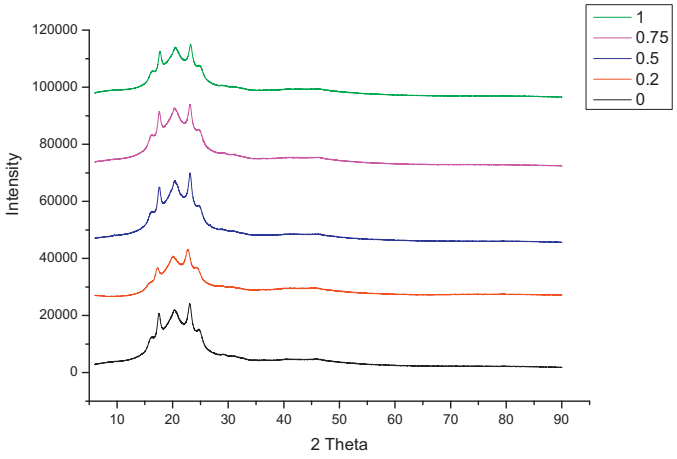

Fig. 3. X-ray diffraction analysis of PBAT-NFC thermograms.

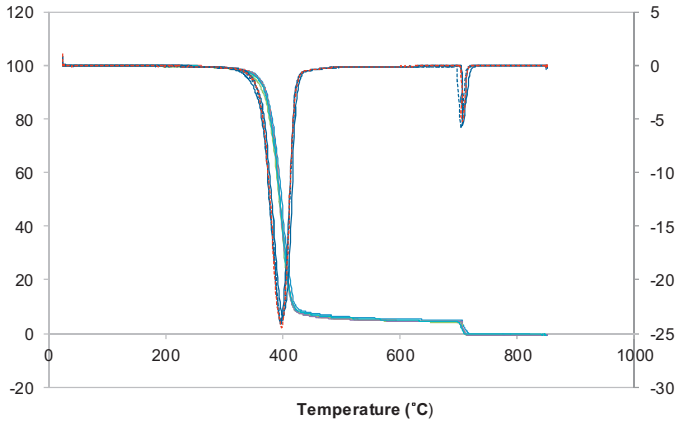

Fig. 4. PBAT-NFC TGA thermograms.

is probably due to optimal dispersion of NFC at 0.2 wt% loading. At higher frequency, this difference is minimized due to the hydrodynamic force. The result is similar to the observation made by Madera-Santana et al. (2009) on NFC-PBAT composite, where at a lower frequency; the influence of agar particle increased the storage modulus. The complex viscosity data showed a shear thinning behavior. As expected, the influence of the NFC filler on the complex viscosity is observed at a lower frequency, when the hydrodynamic force is not very dominant. This enhancement is probably due to the uniform dispersion of NFC in PBAT matrix at 0.2 wt% loading, as observed in the TEM study.

The phase homogeneity in polymer solutions and melts is often derived from Cole-Cole plot where the imaginary part of the complex viscosity η'' is plotted as function of the real part η' (Cole & Cole, 1941; Warren, Schrag, & Ferry, 1973). Generally, in a melt, at very low frequencies solid-like behavior is observed, whereas at higher frequencies liquid-like behavior prevails. In this formation, $G^*(\omega) = G'(\omega) + iG''(\omega)$, a modified Cole-Cole plot can be obtained by plotting G' against G'' (Park, Kim, Choi, & Lee, 2007). Fig. 5(d) represents a modified Cole-Cole plot of PBAT and PBAT-NFC composite using the G' and G'' data from Fig. 5(a) and (b). The plot indicates a shift in the elastic modulus (G') for a loading of 0.2 wt% NFC. This is probably due to the formation of a network structure due to a more homogeneous dispersion. With increasing concentration of NFC (0.5–1.00 wt%), the curve collapsed into a single line with a slope of 1.75. This suggests that there are few structural changes like agglomeration of the filler, as the NFC concentration increased. It will be interesting to note here that the Cole-Cole plot is also complementing the complex viscosity data in Fig. 5(c), where there is an optimal increment of the storage modulus at 0.2 wt% loading of NFC. The observed trend is similar to the trend observed by Park et al. (2007) on polystyrene clay nanocomposite.

It is well known that the storage modulus (G') at low frequency range is more sensitive to the structural changes in the polymer nanocomposites (Mabrouk et al., 2011). Thus the slope of dependence of G', denoted as n', is plotted against different loading of NFC (0.2–1 wt%) at the low frequency range (0.01–1 rad/s) in Fig. 5(e).

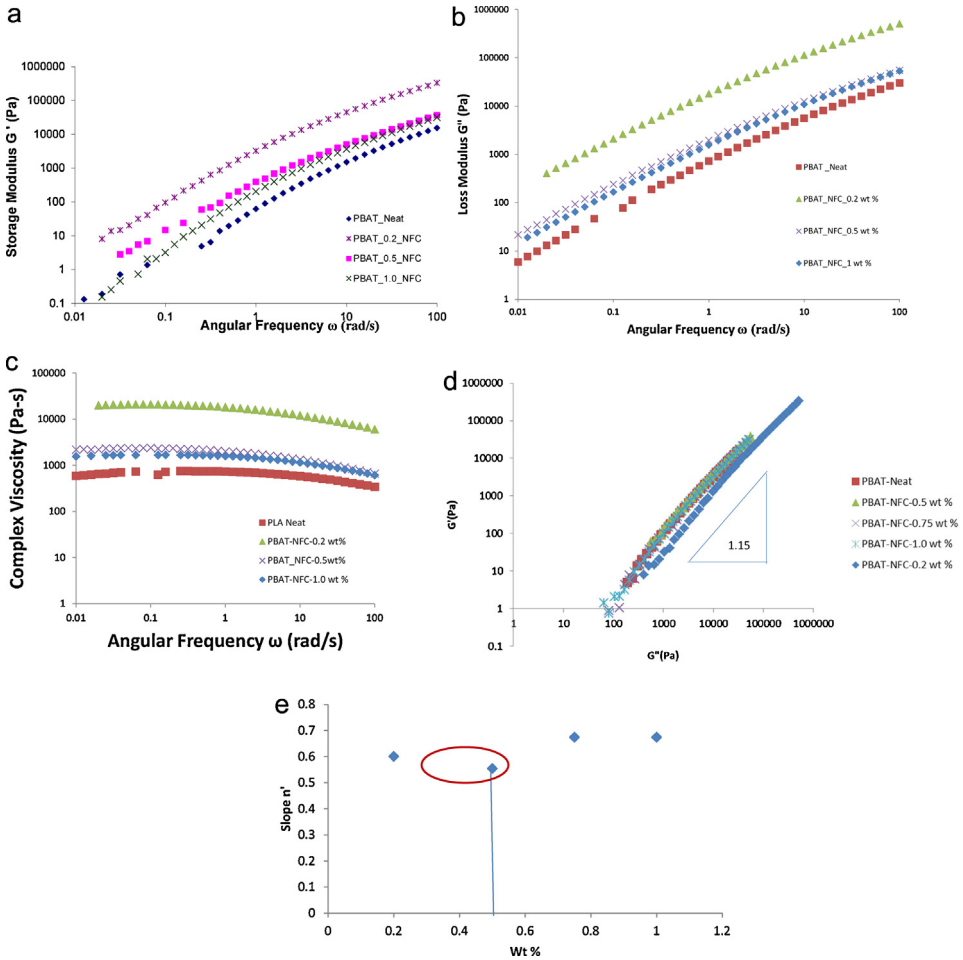

Fig. 5. (a) Comparison of storage modulus (G'). (b) Comparison of loss modulus (G'). (c) Comparison of complex viscosity (η'). (d) Cole–Cole plot. (e) Slope (n') for storage modulus G' at low frequency for PBAT-NFC composites.

This figure evaluates the rheological percolation threshold for a uniform dispersion. From the figure, it is observed that around 0.2–0.5 wt% loading, a region of minimum slope exists and indicates that beyond that region, dispersion is affected by agglomeration. This empirical study is carried out to quantify the degree of dispersion and to evaluate the optimal loading for a uniform dispersion of NFC in PBAT matrix.

3.4. Discussions on dispersion, structure and property

Dispersion is the key factor in improving the strength of the nanocomposites, as homogeneous separation of nanoscale particles is responsible for high interface of contact between the fiber and the matrix. A good fiber matrix adhesion creates a synergistic effect, leading to the overall property improvement of the polymer material. The homogeneous dispersion of NFC in the PBAT matrix is challenging due to the high polarity of the cellulose surface (Ten & Vermerris, 2013). In this study, the degree of dispersion is evaluated my morphological, rheological and thermal tests. TEM analysis indicates an optimal dispersion of PBAT-NFC (0.2 wt%) composite. This uniform dispersion is contributing to the shift of glass transition and crystallinity in DSC and enhancement of storage modulus in shear rheological tests. Notably, the TGA curve shows no deflection meaning that NFC is well dispersed in PBAT or makes up too little of the mass to be detected. A quantitative approach is attempted to evaluate the degree of dispersion by evaluating the rheological percolation threshold. The evaluation indicates a percolation around the region of 0.2–0.5 wt%. Further to the study, Cole-Cole plot suggests a network formation of NFC due to homogeneous dispersion at an optimal loading of 0.2 wt%. Beyond that loading agglomeration and few structural changes are apparent.

4. Conclusions

A series of bio-nanocomposites were developed by reinforcing NFC from regenerated wood fiber into poly(butylene adipate-co-terephthalate) PBAT by injection molding. The incorporation of NFC in PBAT matrix (0.2–1 wt%) increased the storage modulus (G') and dynamic viscosity (η') as revealed by shear rheology, indicating a percolation threshold around 0.2–0.5 wt% region. DSC analysis showed similar improvement with slight improvement of glass transition (T_g) and crystallization temperature (T_c). Percentage crystallinity, as calculated from heat of fusion equation and taking into account 100% crystallized PLA data, reflected an optimal improvement at 0.2 wt% loading. This indicates NFC has a good potential to act a nucleating agent in the PBAT matrix.

Acknowledgments

The authors would like to acknowledge the facilities, and the scientific and technical assistance received from Mr. Phil Francis and Mr. Peter Rummel of the Australian Microscopy and Microanalysis Research Facility at the RMIT Microscopy and Microanalysis Facility, RMIT University; Mr. Frank Antolasic from School of Applied Sciences; Dr. Nurul Quazi, Mr. Mike Allan and Dr. Muthu Panniselvam, from School of Civil, Environmental and Chemical Engineering, RMIT University; Prof. Amar K. Mohanty, Dr. Manjusri Misra, Dr. Murali Reddy and Lauren Surtleff from the University of Guelph, for their continued support in completing the experimental work.

References

Averous, L., & Boquillon, N. (2004). Properties of biocomposites based on lignocellulosic fillers. *Carbohydrate Polymers*, *56*, 111–122.

Bittman, B., Bouza, R., Barral, L., González-Rodríguez, M. V., & Abad, M. J. (2008). Nanoclay-reinforced poly(butylene adipate-co-terephthalate) biocomposites for packaging. *Polymer Composites*, *33*, 2022–2028.

Brinchi, L., Cotana, F., Fortunati, E., & Kenny, J. M. (2013). Production of nanocrystalline cellulose from lignocellulosic biomass: Technology and applications. *Carbohydrate Polymers*, *94*, 154–169.

Chivrac, F., Pollet, E., & Averous, L. (2007). Nonisothermal crystallization behavior of poly(butylene adipate-co-terephthalate)/clay nano-biocomposites. *Journal of Polymer Science Part B: Polymer Physics*, *45*, 1503–1510.

Cole, K. S., & Cole, R. H. (1941). Dispersion and absorption in dielectrics. I. Alternating current characteristics. *Journal of Chemical Physics*, *9*, 341–351.

Couderc, S., Duclouz, O., Kim, B. J., & Soumeya, T. (2009). A mechanical switch device made of a polyamide-coated microfibrillated cellulose sheet. *Journal of Micromechanics and Microengineering*, *19*.

Hubbe, M. A., Rojas, O. J., Lucia, L. A., & Sain, M. (2008). Cellulosic composites: A review. *Bioresources*, *3*, 929–980.

Khalil, H. P. S. A., Bhat, A. H., & Yusra, A. F. I. (2012). Green composites from sustainable cellulose nanofibrils: A review. *Carbohydrate Polymers*, *87*, 963–979.

Lavoine, N., Desloges, I., Dufresne, A., & Brass, J. (2012). Microfibrillated cellulose – its barrier properties and applications in cellulosic materials: A review. *Carbohydrate Polymers*, *90*, 735–764.

Ludvic, C. N., Glenn, G., Klamczynski, A., & Wood, D. (2007). Cellulose fiber/bentonite clay/biodegradable thermoplastic composites. *Journal of Polymers and the Environment*, *15*, 251.

Mabrouk, A. B., Magnik, A., Belgacem, M. N., & Boufi, S. (2011). Melt rheology of nanocomposites based on acrylic copolymer and cellulose whisker. *Composite Science and Technology*, *71*, 818–827.

Madera-Santana, T. J., Drzal, L. T., Robledo, D., & Freile-Pelegrin, Y. (2009). Preparation and characterization of biodegradable agar/poly(butylene adipate-co-terephthalate) composites. *Polymer Engineering and Science*, *49*, 1117–1126.

Moon, R. J., Martini, A., Nairn, J., Simonsen, J., & Youngblood, J. (2011). Cellulosic nanomaterials review: Structure, properties and nanocomposites. *Chemical Society Review*, *40*, 3941–3994.

Park, B. J., Kim, T. H., Choi, H. J., & Lee, J. H. (2007). Emulsion polymerized polystyrene/montmorillonite nanocomposite and its viscoelastic characteristics. *Journal of Macromolecular Science Part B: Physics*, *46*, 341–354.

Raquez, J. M., Nabar, Y., Narayan, R., & Dubois, P. (2008). Novel high-performance talc/poly[(butylene adipate)-*co*-terephthalate] hybrid materials. *Macromolecular Material Engineering*, *293*, 310–320.

Siro, I., & Plackett, D. (2010). Microfibrillated cellulose and new nanocomposite materials: A review. *Cellulose*, *17*, 459–494.

Ten, E., & Vermerris, W. (2013). Functionalized polymers from lignocellulosic biomass: State of the art. *Polymers*, *5*, 600–642.

Warren, T. C., Schrag, J. L., & Ferry, J. D. (1973). Infinite-dilution viscoelastic properties of poly-γ-benzyl-L-glutamate in helicogenic solvents. *Biopolymers*, *12*, 1905–9015.

Wu, C.-S. (2012). Characterization of cellulose acetate-reinforced aliphatic aromatic copolyester composites. *Carbohydrate Polymers*, *87*, 1249–1256.

Yano, H., & Nakahara, S. (2004). Bio-composites produced from plant microfiber bundles with a nanometre unit web-like network. *Journal of Materials Science*, *39*, 1638–1653.

Yano, H., Sugiyama, J., & Nakagaito, A. N. (2005). Optically transparent composites reinforced with networks of bacterial nanofibres. *Advanced Materials*, *17*, 153–155.

Zadorecki, P., & Michell, A. J. (1989). Future prospects of wood cellulose as reinforcement in organic polymer composites. *Polymer Composites*, *10*, 69–77.